Korean J. Chem. Eng., 37(11), 2054-2063 (2020)
DOI: 10.1007/s11814-020-0585-3

pISSN: 0256-1115
eISSN: 1975-7220

Superwetting TiO_2-decorated single-walled carbon nanotube composite membrane for highly efficient oil-in-water emulsion separation

Yahong Sun*, Ruiguang Zhao, Quanyong Wang***, Yuanyuan Zheng*, Gongrang Li****, Dejun Sun**, Tao Wu**,†, and Yujiang Li*,†**

*Shandong Provincial Research Center for Water Pollution Control, School of Environmental Science and Engineering, Shandong University, Jinan, 250100, P. R. China
**Key Laboratory of Colloid and Interface Science of Education Ministry, Shandong University, Jinan, 250100, P. R. China
***China Urban Construction Design & Research Institute Co. LTD. Jinan, 250101, P. R. China
****Drilling Technology Research Institute, Shengli Petroleum Engineering Corporation Limited of SINOPEC, Dongying, 257017, P. R. China

(*Received 5 January 2020 • Revised 9 May 2020 • Accepted 20 May 2020*)

Abstract−With the advantages of one-dimensional hollow structure, high porosity and prominent mechanical strength, single-walled carbon nanotubes (SWCNTs) have been extensively utilized to improve conventional filtration membranes for oil/water separation. Their intrinsic hydrophobicity, however, adversely affects the anti-fouling performance of the SWCNT membrane. Herein, a super-hydrophilic and underwater super-oleophobic hierarchical modified membrane with enhanced permeability and anti-fouling property was fabricated using the vacuum-assisted filtration technique by synergistically assembling SWCNTs and titanium dioxide (TiO_2) nanoparticles on a cellulose acetate membrane. Highly dispersed SWCNTs were obtained by carboxylating treatment of agglomerate SWCNTs. The controlled stacking of SWCNTs fibers and a controllable amount of TiO_2 rendered a modified membrane with high porosity and hierarchical structure, leading to an ultrahigh water flux up to 4,777.07 $L \cdot m^{-2} \cdot h^{-1}$, and excellent separation performance with efficiency greater than 99.47%. Most importantly, the membrane exhibited excellent anti-fouling ability during ten cycles with the aid of the super-wetting property of TiO_2 nanoparticles. The results indicated that coating TiO_2 nanoparticles on SWCNTs modified the surface topography of the obtained SWCNT/TiO_2 membrane, which improved hydrophilicity, permeability and anti-fouling property, manifesting attractive potential applications in oil/water separation.

Keywords: Oil-in-water Emulsions, Super-hydrophilic, Underwater Super-oleophobic, SWCNT/TiO_2 Membranes, SWCNT Membrane

INTRODUCTION

With the increasing release of oily industrial wastewater and the frequency of oil spills, oil/water separation problems have attracted considerable public attention [1-3]. Direct discharge of oily wastewater can damage the ecosystem and seriously endanger human health [4,5]. Traditional techniques such as sedimentation tanks, air flotation, ultrasonic separation, centrifuges, coalescers, and skimmers have been utilized to treat oily wastewater [6-8]. However, these techniques are only suitable for the treatment of immiscible oil/water mixtures; for surfactant-stabilized oil-in-water emulsions with a droplet size less than 10 μm, they are essentially ineffective [9-12]. For oil/water emulsions, filtration and adsorption are often used. Due to the poor selectivity of adsorption materials for oil and water, however, they adsorb the oil/water mixture, resulting in poor oil/water separation efficiency. In addition, adsorption materials are not easy to recycle, and the post-treatment process results in serious secondary pollution [13]. The separation effects of several adsorbents and membrane materials are compared (Table S1) [14-17].

The utilization of membrane technology provides a potential solution for microsized oily wastewater [18]. It has been acknowledged that membrane technology can reject micron-sized particles and molecules due to its molecular sieving effect, coupled with its unique surface properties and surface structure, and has been successfully applied for the separation of various emulsions [19,20]. Moreover, owing to its green and simple operation, and energy-efficient and continuous operation advantages, membrane technology has been extensively employed for oil/water separation [21-23]. However, traditional commercial membranes, such as CA, PES and PVDF, are susceptible to serious oil fouling caused by surfactant/oil adsorption or pore plugging, which results in membrane fouling and high costs for large effluent volumes [24-26]. Indeed, numerous research groups have fabricated composite membranes for oil/water separation. Hydrophobic membranes used to treat oil-in-water emulsions, however, can cause severe membrane contamination due to oil adhesion [27-29]. Currently developed hydrophilic membranes suffer from low flux and poor separation efficiency, which seriously limits applications of the membranes [30-32]. Consequently, a great need exists for new, advanced separation membranes that are capable of working with superior permeation and oil rejection [33,34].

Due to their excellent mechanical, thermal, and chemical prop-

†To whom correspondence should be addressed.
E-mail: yujiang@sdu.edu.cn, wutao@sdu.edu.cn

erties, carbon nanotubes (CNTs) offer numerous potential applications, including field emission displays, nano-electronic devices, and polymer or ceramic reinforcement [35]. Moreover, their high surface area, good chemical stability, high porosity and low density make them an ideal participant in the treatment of oily wastewater [36]. Single-walled carbon nanotubes (SWCNTs) can also achieve extremely high permeation flux owing to their one-dimensional hollow structure and prominent mechanical strength [37-39]. Unfortunately, the inherent hydrophobicity of carbon nanotubes is prone to cause membrane fouling, resulting in a rapid decline in permeate flux, as well as secondary pollution, which is incongruous for large-scale oil/water separation operations. Consequently, it is necessary to carry out carboxylation treatment, in addition to adding hydrophilic substances to further increase surface wettability.

Inspired by fish scales, "water-removing" membranes with superhydrophilicity and underwater super-oleophobicity have attracted widespread focus because they can remain clean as long as they are water-wetted [40]. Various hydrophilic materials, such as polymers and inorganic metal oxides, have been considered to prepare "water-removing" membranes [41]. Polymers such as hydrogel usually exhibit weak environmental adaptability, while inorganic nanoparticles in the membrane matrix can practically improve mechanical strength, hydrophilicity, water flux, and anti-fouling properties [42,43]. Among them, nanosized titanium dioxide (TiO_2) is a superior candidate as an additive due to its strong adhesion, stable chemical properties, low cost, green, and environmentally benign aspect [44]. Titanium and oxygen atoms in titanium dioxide are located in the crystal lattice, and Ti-O bonds are not equal in length and close in distance. The imbalance between Ti-O bonds makes TiO_2 possess strong polarity and water retention capacity. The water molecules adsorbed on the surface are dissociated due to polarization to form hydroxyl groups. Studies have demonstrated that the larger the specific surface area of TiO_2 particles, the more hydroxyl groups it carries on its surface, and the presence of abundant hydroxyl groups leads to concurrent smooth water filtration and prominent oleophobicity [45,46]. Therefore, TiO_2 nanoparticles are utilized as a key inorganic additive material to modulate the wettability of the SWCNT membrane surface, which greatly alleviates membrane fouling. Jin's group fabricated a novel film by coating TiO_2 via the sol-gel process onto an SWCNT ultrathin network film [47]. However, the super-hydrophilic and underwater super-oleophobic properties of this film can only be achieved by employing UV-light irradiation. Consequently, to develop a high mechanical strength membrane which can be easily prepared, have continuous super-hydrophilic and underwater super-oleophobic properties and be energy-efficient is of paramount significance.

In this work, aiming at simultaneously improving water permeability and anti-fouling performance of cellulose acetate (CA) membrane for feasible application of ultrafast oil/water separation, we constructed superhydrophilic-superoleophobic surfaces in conjunction with surface chemistry and structure. It is expected that coating TiO_2 nanoparticles on SWCNTs fibers can expand the channel structure and modify the surface topography of the membrane, resulting in high permeation flux and hierarchical structure. Moreover, abundant surficial hydroxyl groups endow the composite membrane with high water retention capacity and greater hydrophilicity. And the synergistic effect of the modified surface chemistry and surface architecture is anticipated to facilitate the permeation flux and anti-fouling behavior of the SWCNT-based membrane. The resulting modified SWCNT/TiO_2 composite membrane is predicted to maintain high permeation flux and high separation efficiency during multiple cycles, demonstrating excellent anti-fouling performance. The present work may contribute substantially to treating real emulsions.

EXPERIMENTAL

1. Materials

Cellulose acetate (CA) microfiltration membrane (0.45 μm pore size, 47 mm diameter) from the Safelab Technology Co., Ltd. (Beijing, China) was used as the support layer for modification. The SWCNTs (o.d. <2 nm, length: 1-3 μm, purity: >95%) utilized in this study were a commercial product supplied by the Nanjing XFNANO Materials Tech Co., Ltd. (Nanjing, China). TiO_2 nanoparticles (anatase, hydrophilic, 60 nm, 99.8%) were obtained from the Macklin Biochemical Technology Co., Ltd. (Shanghai, China). Decane (Acros Organics BVBA, Geel, Belgium), hexadecane (Tokyo Chemical Industry Co., Ltd., Tokyo, Japan), white mineral oil (Marcol 52) (Exxon Mobil Co, Ltd., Avon, U.S.A.), and petroleum ether (Sinopharm Chemical Reagent Co., Ltd., Shanghai, China) used for oil-in-water emulsions preparation were purchased. Sodium dodecyl benzene sulfonate (SDBS) was supplied by the Shanghai National Medicines Co., Ltd. (Shanghai, China). Deionized water (>18.2 MΩ cm^{-1}), which was used throughout the experiment, was purified by the Persee GW purification system (Beijing, China). All chemicals used in the experiments were of reagent grade.

2. Fabrication of the SWCNT and SWCNT/TiO_2 Modified Membranes

Original SWCNTs have very poor dispersion in deionized water due to their intrinsic hydrophobic property. To improve dispersibility, carboxylation pretreatment of SWCNTs is indispensable. Ultra-high purity carboxylated SWCNTs could be generated by nitric/sulfuric acid treatment.

The SWCNT membrane and the SWCNT/TiO_2 modified membrane were separately prepared by vacuum filtering the SWCNT dispersion and the SWCNT/TiO_2 mixture onto a CA filter with a pore size of 0.45 μm. Typically, 5 mg of ultra-high purity carboxylated SWCNTs were dispersed in water in a 200 mL beaker and sonicated for 10 min. TiO_2 nanoparticles (anatase) were then added into the prepared SWCNTs suspension under stirring to obtain the mixture of TiO_2 and SWCNTs with mass ratios that varied from 1 to 7. The specific percentage of TiO_2 coated SWCNTs, with a different mass ratio of TiO_2 and SWCNTs (0 : 1, 1 : 1, 3 : 1, 5 : 1, and 7 : 1, respectively), were dispersed by sonication for an additional 10 min to improve the homogeneity. Afterwards, the obtained SWCNTs and SWCNTs/TiO_2 suspensions were vacuum-filtered upon the CA membrane to obtain SWCNT membrane and SWCNT/TiO_2 membranes. Subsequently, the prepared membrane samples were rinsed with deionized water and then dried in a vacuum drying oven at 313 K for 5 h.

3. Preparation of Oil-in-water Emulsions

The SDBS-stabilized oil-in-water emulsions, including hexadec-

ane-in-water, white oil-in-water, decane-in-water, and petroleum ether-in-water emulsions with droplet diameter of 1.38, 1.55, 1.70, and 1.91 μm, respectively, were prepared. For the preparation, 1.5 g of oil was added to 1 L of water. SDBS with a concentration of 50 mg/L was added to the mixture as an emulsifier. The mixture was stirred at 10,000 rpm for 10 min to obtain a white milky solution. All of the surfactant-stabilized oil-in-water emulsions were stable for several hours in a laboratory environment and no demulsification or precipitation was observed. All emulsions were separated immediately after preparation.

4. Characterization of Membranes

Fourier transform infrared spectroscopy (FTIR) (Nicolet Nexus 670, Thermo Fisher Scientific, U.S.A.) with an attenuated total reflectance (ATR) accessory was utilized to confirm the covalent structure of the modified membrane surface. Membrane surface morphology and cross-section were observed with field-emission scanning electron microscopy (SEM) (SU8010, Rili, Japan). Atomic force microscopy (AFM) (Dimension ICON, Bruker, U.S.A.) was applied to evaluate the surface roughness. Contact angles were measured on the Teclis Tracker tensiometer platform at ambient temperature. For each value, three measurements per sample were performed and the average value was obtained. In the process of the underwater oil contact angles (UOCA) experiment, all membranes were fixed at the bottom of a special quartz tank filled with water, and 1, 2-dichloroethane was used as a model oil because its density is larger than water and is easy to deposit at the bottom of the aqueous phase and contact with the membrane. The simulated drag force test was carried out using an approach-compress-detach of a 1, 2-dichloroethane droplet (3 μL). The oil content in the corresponding collected filtrates was determined using an infrared oil detector (OIL 460, China). Oil droplet size of four different oil-in-water emulsions was measured by dynamic light scattering (DLS) (BI-200SM, Brookhaven, U.S.A.).

5. Oil-in-water Emulsions Separation

The modified membrane was previously wetted with water and then fixed by a vacuum-driven filtration system with an effective permeation area of 12.56 cm^2 under 0.1 MPa trans-membrane pressure. 50 mL of the oil-in-water emulsion was poured onto the membrane to perform oil/water separation. The flux was evaluated along with the filtration process by calculating the time of emulsion penetrating through the membrane. The filtrate was collected for subsequent measurement of the oil content. In one cycle of the anti-fouling performance experiment, 50 mL of the white mineral oil-in-water emulsion was completely separated by the modified membrane, and then the membrane was simply rinsed with pure water to remove oil contamination. Each membrane was measured in triplicate to ensure high reproducibility of this measurement. The permeation flux (J) was calculated by Eq. (1). The separation efficiency (R) characterized by oil rejection ratio was calculated by Eq. (2):

$$J = \frac{V}{A \times \Delta t} \tag{1}$$

$$R = \left(1 - \frac{C_p}{C_o}\right) \times 100\% \tag{2}$$

where J is the permeation flux ($L \cdot m^2 \cdot h^{-1}$); V is the volume of feed emulsion (L); A is the efficient membrane area (m^2); Δt is the permeation time (h); and C_o and C_p are the concentrations of the oil in the original and permeate solutions, respectively.

6. Porosity

Membrane porosity was determined by the dry-wet weight method [48]. The membrane was immersed in water, and then filter paper was used to wipe off the superficial water. The weight was recorded in the wet state. Next, the wetted membrane was placed in a vacuum drying oven at 313 K for 24 h before measuring the dry weight. The porosity (ε) was determined as defined by Eq. (3):

$$\varepsilon = \frac{m_w - m_d}{A \times \delta \times \rho_w} \tag{3}$$

where ε is the porosity of membrane, m_w and m_d are the wet and dry sample weight (g), respectively; ρ_w is the density of pure water (g/cm^3); A is the area of membrane in wet state (cm^2); and δ is the

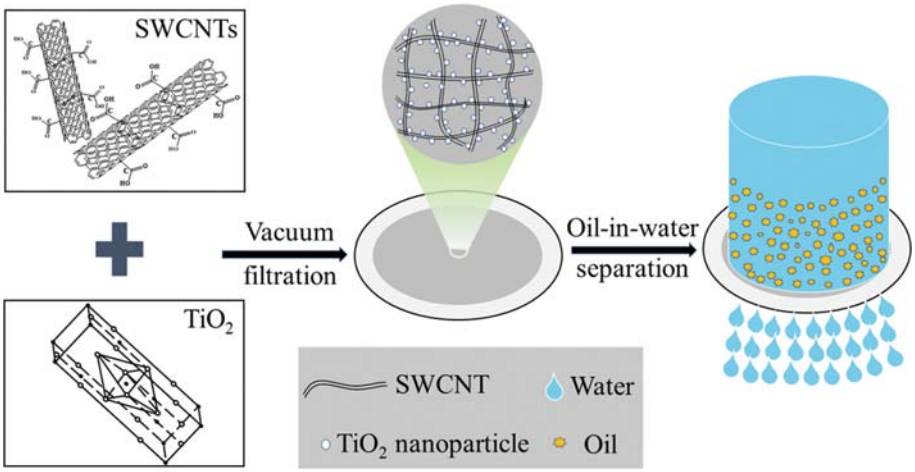

Fig. 1. Schematic illustration of the fabrication of SWCNT/TiO_2 membrane via vacuum-assisted filtration and the separation of an oil-in-water emulsion.

membrane thickness by SEM characterization (cm). Each membrane was measured in triplicate to obtain an average value.

RESULTS AND DISCUSSION

1. Membrane Fabrication and Characterization

A series of SWCNT/TiO_2 modified membranes were fabricated by combining the nano-properties of TiO_2 with the special geometrical structure of SWCNTs, and the mass ratio of TiO_2 to SWCNTs was controlled by changing the additive amount of TiO_2 during the modification process. The fabrication procedure of SWCNT/TiO_2 modified membrane via vacuum-assisted filtration assembly is schematically presented in Fig. 1. The bare SWCNTs tend to agglomerate through strong van der Waals forces [49]. However, due to the oxidation treatment and subsequent sonication, the SWCNTs are not intertwined with each other. The ultra-high purity carboxylated SWCNTs used in this study were made by nitric/sulfuric acid oxidation treatment. There were abundant carboxylic acid groups on the surface of SWCNTs, which could have polar covalent bonding by the electro-negativity difference [42]. TiO_2 is positively charged at a pH of 7, and it can adhere well to the CA membrane. Moreover, TiO_2 nanoparticles are attached to SWCNTs by surface adsorption and covalent bonding [50,51]. The surface adsorption results from the electrostatic attraction between the carboxyl groups on the SWCNT surface and titanium ions [52]. Chemical adsorption is ascribed to the strong interaction between carboxyl groups and TiO_2, such as ester-like linkages and hydrogen bonding [53,54].

To elucidate the composites of the membrane surface, FTIR analysis was performed to investigate the surface functional groups. To further confirm the ultra-high purity carboxylation of SWCNTs, FTIR spectra of SWCNTs are shown in Fig. S1. The SWCNT particles exhibit a broad and strong characteristic peak at ~3,409 cm^{-1} that can be ascribed to the O-H bond stretching of hydroxyl, because the oxidized SWCNTs possessed abundant carboxyl groups. There are also obvious stretching vibration bands of C=O at ~1,747 cm^{-1} and ~1,566 cm^{-1}. In addition, the bond at ~1,186 cm^{-1} is attributed to C-O vibration. Fig. 2 shows the FTIR spectra of the CA membrane, SWCNT coated membrane, and SWCNT/TiO_2 coated membranes. The CA membrane has characteristic bands at ~3,492 cm^{-1} and ~1,745 cm^{-1}, which are attributed to O-H stretching and C=O stretching, respectively. There are also evident C-H vibration peaks at ~2,940 cm^{-1} and ~2,883 cm^{-1}. The C-O stretching of carboxylic groups and the C-O-C bridge asymmetric stretching appear at

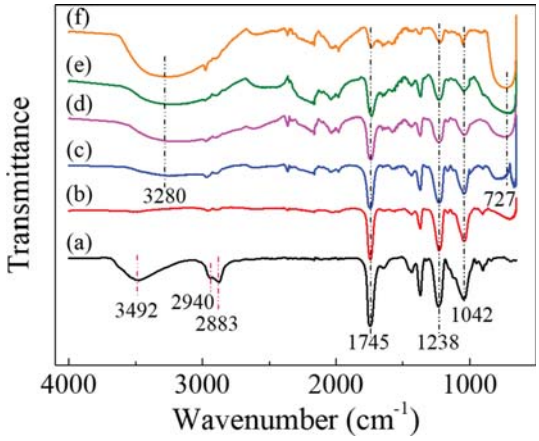

Fig. 2. ATR-FTIR spectra of (a) pure CA membrane, (b) SWCNT membrane, (c) SWCNT/TiO_2 membrane (TiO_2/SWCNT=1), (d) SWCNT/TiO_2 membrane (TiO_2/SWCNT=3), (e) SWCNT/TiO_2 membrane (TiO_2/SWCNT=5), and (f) SWCNT/TiO_2 membrane (TiO_2/SWCNT=7).

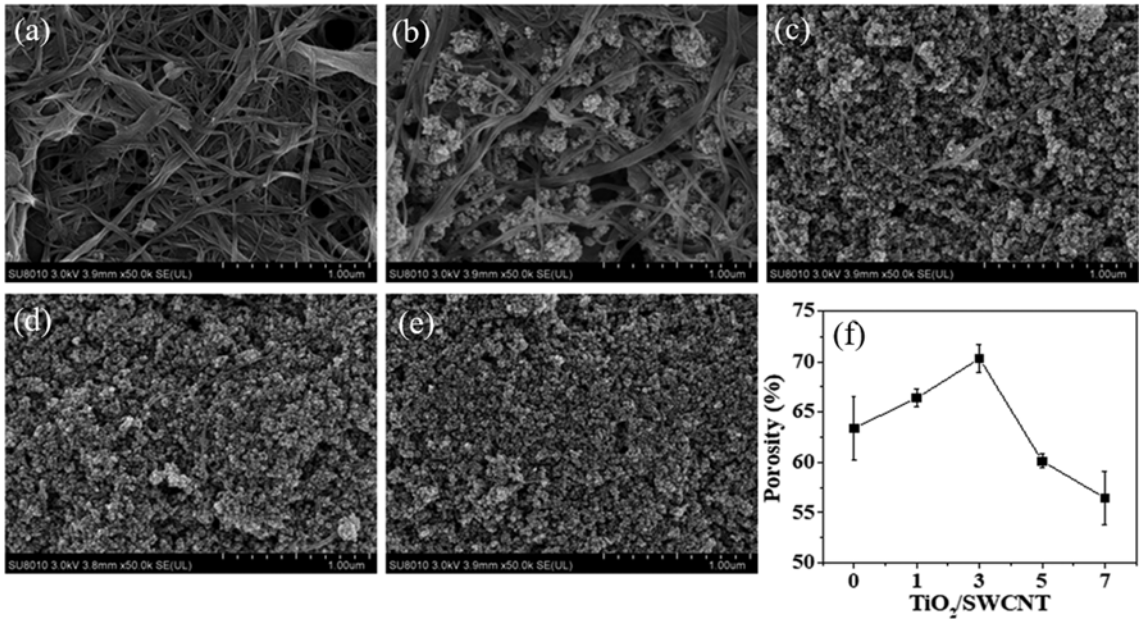

Fig. 3. SEM images of (a) SWCNT membrane, (b) SWCNT/TiO_2 membrane (TiO_2/SWCNT=1), (c) SWCNT/TiO_2 membrane (TiO_2/SWCNT=3), (d) SWCNT/TiO_2 membrane (TiO_2/SWCNT=5), and (e) SWCNT/TiO_2 membrane (TiO_2/SWCNT=7). (f) Porosity of modified membranes with various nano-TiO_2 contents.

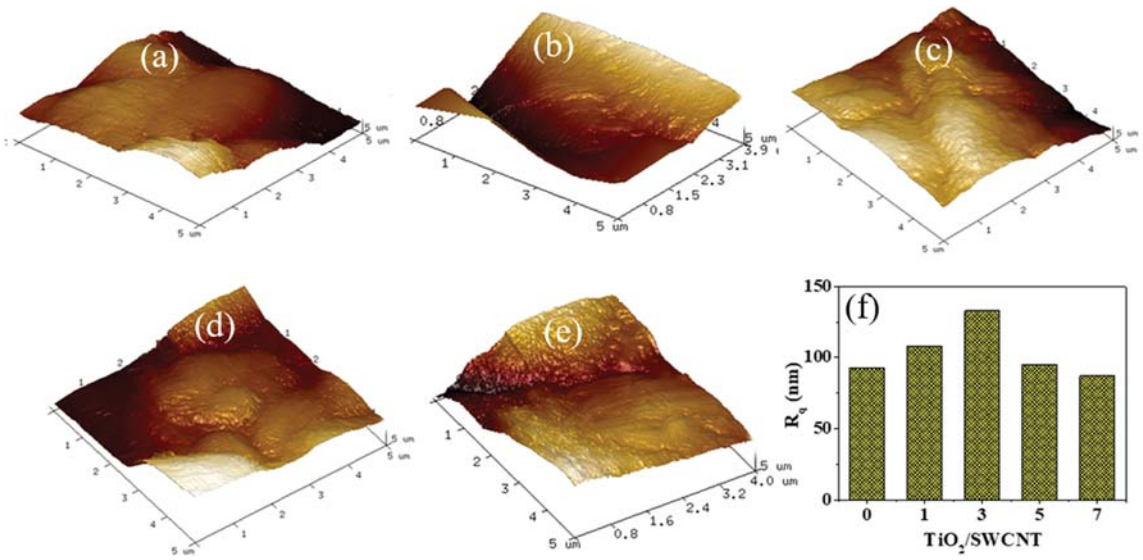

Fig. 4. 3D AFM images of (a) SWCNT membrane, (b) SWCNT/TiO_2 membrane (TiO_2/SWCNT=1), (c) SWCNT/TiO_2 membrane (TiO_2/SWCNT=3), (d) SWCNT/TiO_2 membrane (TiO_2/SWCNT=5), and (e) SWCNT/TiO_2 membrane (TiO_2/SWCNT=7). (f) R_q values of membranes with different TiO_2/SWCNT mass ratios.

~1,238 cm^{-1} and ~1,042 cm^{-1}, respectively. When SWCNTs were deposited on the CA membrane, the characteristic peak of O-H was not obvious when the transmittance range was large due to the poor transmittance of SWCNTs to infrared light. When TiO_2 was deposited on the SWCNTs fiber, significant changes in the characteristic peaks of the membrane surface were observed, indicating that TiO_2 altered the chemical composition of the membrane surface. The shift of the O-H vibration band from ~3,492 cm^{-1} to ~3,280 cm^{-1} and the increasingly obvious peak vibration caused by an increase in the amount of TiO_2 both constitute evidence that more hydrogen bonds were formed in the membrane surface. Furthermore, the modified membrane exhibits a distinct broad peak at ~727 cm^{-1}, which is ascribed to the Ti-O vibration caused by the adhesion of TiO_2 nanoparticles to the SWCNTs fiber. These results demonstrate that TiO_2 nanoparticles are successfully loaded onto single-walled carbon nanotubes.

The surface morphologies of CA membrane, SWCNT membrane, and SWCNT/TiO_2 membranes were investigated by SEM. The CA membrane exhibited a porous structure and was relatively smooth compared with modified membranes (Fig. S2(a)). As shown in Fig. 3(a), SWCNTs were coated on the base membrane surface loosely with single SWCNT stacked together. The SWCNT membrane is relatively flat compared to the SWCNT/TiO_2 membrane. After the addition of TiO_2, TiO_2 nanoparticles were uniformly dispersed between SWCNTs to enlarge the pore size of the SWCNT membrane, and some micro/nanostructures were formed on the membrane surface (Fig. 3(b) and 3(c)). This result constitutes evidence that TiO_2 was successfully embedded between SWCNTs and formed its surface layer to enhance the mechanical strength and hydrophilicity of the membrane. When the mass ratio of TiO_2/SWCNT was increased to 5, the membrane surface was completely covered by hydrophilic TiO_2 nanoparticles and became relatively smooth. With a further increase in the concentration of TiO_2, it could be seen that the surface of the modified membrane exhibited no significant change, and it had become flatter (Fig. 3(e)). Meanwhile, the thickness of the membrane increased slightly, which could be determined by SEM images using image analysis software with more than 5 positions for each membrane, and the porosity increased first and then decreased (Fig. 3(f)). Both were essential to the demulsification of oil-in-water emulsions.

AFM was utilized to obtain intuitive information about hierarchical structures, which are crucial in controlling the anti-fouling behavior of the membranes (Fig. 4). A porous CA membrane was selected as the support for the coating materials. The root-mean-square roughness (R_q) of the pure CA membrane was 89 nm (Fig. S2(b)). When SWCNTs were deposited on the original CA membrane, R_q was slightly increased. It is shown that the load of SWCNTs augmented the roughness of the modified membrane, but still exhibited a relatively flat surface. On a modified membrane coated only with carboxylated SWCNTs, because of low electrostatic interactions among the SWCNTs, they are regularly collocated on the membrane to smooth the surface of the membrane. The R_q of the SWCNT membrane increased from 93 to 108 nm and 133 nm for the SWCNT/TiO_2 membrane (TiO_2/SWCNT=1) and the SWCNT/TiO_2 membrane (TiO_2/SWCNT=3), respectively. Due to the addition of TiO_2 nanoparticles, the surface of the SWCNT/TiO_2 membrane became rough. In addition, as the amount of TiO_2 on SWCNTs increased, the membrane had a higher surface roughness than the SWCNT/TiO_2 membrane (TiO_2/SWCNT=1). Because more loading of TiO_2 on the SWCNTs made the modified membrane flatter, as well as the robust interactions between the two components, the R_q value decreased to 95 nm for the SWCNT/TiO_2 membrane (TiO_2/SWCNT=5). As we further increased the TiO_2/SWCNT mass ratio to 7, the surface roughness of the modified membrane was further reduced with the R_q value of 87 nm. This change is also consistent with the surface morphology described by the SEM. Indeed, it has been reported that an increase in the surface roughness is responsible for the formation of hydrophilicity as well as super-

oleophobicity underwater in the water/membrane interface [55].

2. Wetting Behavior

Increasing the surface roughness can facilitate the formation of super-hydrophilic and super-oleophobic surfaces because the membrane surface can solidify a part of the water molecules into its hierarchical structure, thereby forming a hydration layer, which can avoid oil droplets from direct contact with the membrane surface and facilitate the demulsification of oil-in-water emulsions [32]. Therefore, it can be inferred that separation performance and anti-fouling properties are highly dependent on the wetting behavior of the membrane surface.

To characterize the surface wettability by hydrophilicity in air and oleophobicity in water of the modified membranes, a series of contact angles were measured. Our previous work demonstrated that the water contact angle of the pure CA membrane could not be measured after 2 s because of the microporous structure [24]. The results of water contact angle (WCA) and underwater oil contact angle (UOCA) of the SWCNT and SWCNT/TiO_2 membranes are shown in Fig. 5. Compared with the hydrophobicity of bare SWCNTs, the hydrophilicity of ultra-high purity carboxylated SWCNTs was increased evidently due to the abundant carboxyl groups formed by the oxidation of strong acid. The WCA of the SWCNT membrane was 32.2°±1.5°, which is unfavorable for emulsion separation (Fig. 5(a)). The WCA of membranes decreased with the addition of TiO_2, implying that the hydrophilic characteristic of nanoparticles made the membrane surfaces more hydrophilic. It can also be seen that the WCA was less than 10° within 2 s, corresponding to the TiO_2/SWCNT mass ratio of 3, 5 and 7, suggesting super-hydrophilicity in air.

Since the as-prepared membranes were mainly used in an aqueous environment, the underwater oil contact angle also constituted a key parameter. Fig. 5(b) shows that the UOCA of the SWCNT membrane was 106.5°±1.6° and oil droplets can easily adsorb on the surface of the membrane, which cannot meet the requirements of oil-in-water emulsion separation. When the mass ratio of TiO_2/SWCNT was 1, the UOCA was 131.2°±2.1°, which is not conducive to the anti-fouling properties of the membrane. As the amount of TiO_2 nanoparticle coating increased, the SWCNT/TiO_2 composite membranes showed an improved underwater oleophobicity with UOCA of 153.4°±3.5°, 157.6°±2.2° and 165.2°±2.5°, corresponding to the TiO_2/SWCNT mass ratio of 3, 5 and 7, respectively. In aggregate, the underwater oil contact angle increased as the TiO_2/SWCNT mass ratio increased. It is obvious that super-hydrophilicity (WCA<10°) and underwater super-oleophobicity (UOCA>150°) of SWCNT/TiO_2 membrane were achieved by coating an appropriate amount of hydrophilic TiO_2 nanoparticles on SWCNTs. Moreover, owing to the hierarchical structures, more water would be entrapped in the membrane pores to form a robust

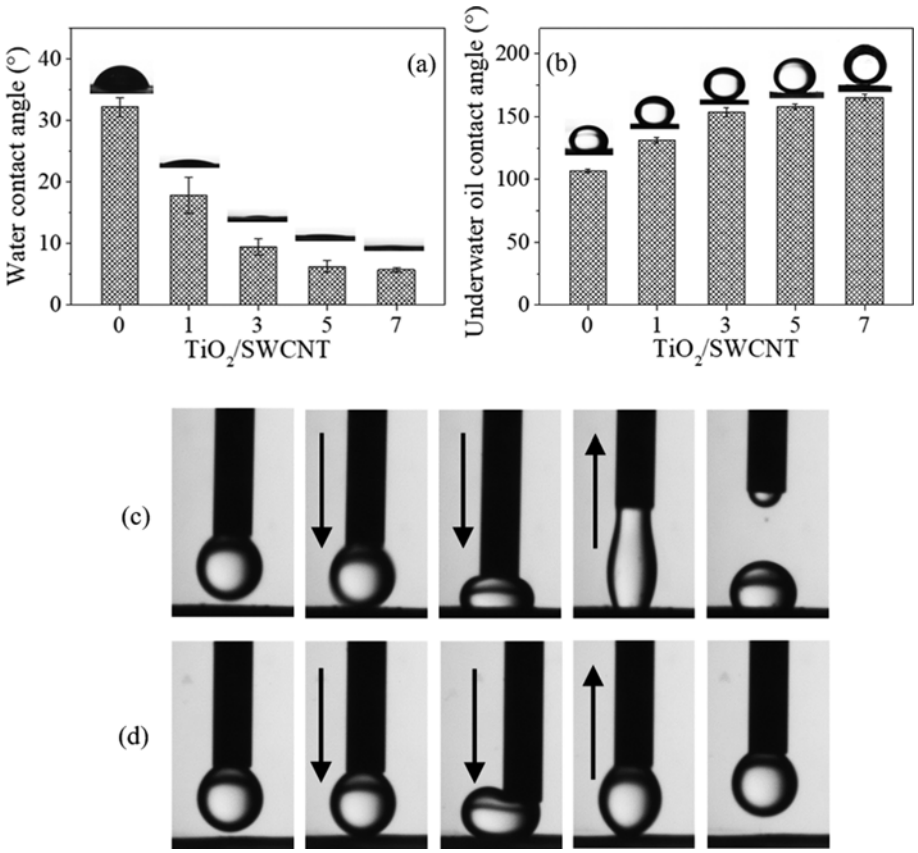

Fig. 5. Water contact angle in air (a) and underwater oil contact angle (b) of SWCNT/TiO_2 membranes with different TiO_2/SWCNT mass ratios. Photographs of dynamic measurements of oil-adhesion under water of the (c) SWCNT membrane and (d) SWCNT/TiO_2 membrane (TiO_2/SWCNT=3).

hydration layer, which can avoid direct contact between oils and membrane surfaces. Overall, as the surface hydration capacity increased, the underwater oil contact angle also increased.

To further elucidate the oil repellency of the two different modified membranes, the SWCNT membrane and SWCNT/TiO_2 membrane (TiO_2/SWCNT=3) were submitted to an underwater adhesion test. Fig. 5(c) and 5(d) show dynamic photographs, in which a 3 μL oil droplet was forced to touch the surface of the SWCNT membrane and SWCNT/TiO_2 membrane and then lifted up. The obvious deformation of the oil droplet proved that it was in full contact with the membrane surface. Consequently, as the oil droplet was lifted off of the SWCNT membrane, the oil droplet formed an elliptical shape due to adhesion to the membrane surface and eventually remained on the membrane. However, due to the lower adhesion of the oil droplet to the membrane surface, the oil droplet could overcome the adhesive force, which facilitated the detachment of the oil droplet from the SWCNT/TiO_2 (TiO_2/SWCNT=3) membrane. For the hierarchical SWCNT/TiO_2 (TiO_2/SWCNT=3) membrane, the trapped water barrier layer effectively prevented oil contact with the membrane. It could efficiently increase the anti-fouling properties and ensure long-term operational stability of separation efficiency.

3. Separation Performance and Anti-fouling Properties

Due to the hierarchical structure and superwetting behavior, water molecules in the emulsion could be selectively adsorbed or permeated through the SWCNT/TiO_2 membrane, resulting in effective and fast separation of surfactant-stabilized oil-in-water emulsions with different oil phases. The flux and separation efficiency of the SWCNT/TiO_2 membrane for SDBS-stabilized hexadecane-in-water emulsion are shown in Fig. 6(a). It can be seen that the SWCNT/TiO_2 (TiO_2/SWCNT=3) had the highest flux of 4,777.07 $L \cdot m^{-2} \cdot h^{-1}$, and the oil rejection could reach 99.47%. This flux value is one order of magnitude higher than commercial filtration membranes with similar rejection properties [11,56,57]. As the mass ratio of TiO_2/SWCNT increased to 5 and 7, respectively, the oil repellency of the modified membranes gradually increased to 99.58% and 99.66%, while the flux decreased to 2,866.24 $L \cdot m^{-2} \cdot h^{-1}$ and 2,388.53 $L \cdot m^{-2} \cdot h^{-1}$. The Hagen-Poiseuille equation ($J = \varepsilon \pi r_p^2 \Delta p / 8 \mu L$) could be used to analyze the flux of liquid through an open pore, by the liquid passing through the membrane, where the flux J is proportional to pore size r_p and surface porosity ε and inversely proportional to membrane thickness L [58]. As the loading of TiO_2 increases, the membrane thickness increases and its pore diameter decreases. It can also be seen from Fig. 3(f) that the surface porosity was 69.80%, 60.83% and 53.88% for TiO_2/SWCNT membranes of 3, 5, and 7 mass ratio, respectively. Therefore, with the increase of TiO_2/SWCNT mass ratio from 3 to 7, the flux gradually decreased. This result was also consistent with the surface roughness results shown in Fig. 4 and contact angles shown in Fig. 5(a) and 5(b).

The oil repellency of all SWCNT/TiO_2 membranes was higher than 98%. These results indicate that oil-in-water emulsions could be successfully separated by SWCNT/TiO_2 modified membranes. Note that 50 mL oil-in-water emulsion cannot penetrate and pass through the pure CA membrane, indicating its poor anti-fouling performance. The SWCNT/TiO_2 (TiO_2/SWCNT=3) membrane was selected as a suitable sample to compare the flux and separation efficiency with the SWCNT modified membrane. Fig. 6(b) shows the separation results of two modified membranes for four different oil-in-water emulsions. The SWCNT membrane has lower oil repellency than the SWCNT/TiO_2 membrane, and the flux is only approximately one-half of that of the SWCNT/TiO_2 membrane. It is well known that the oil-in-water separation mechanism of microfiltration membranes is the molecular sieve effect. The micro-aperture of the membrane acts as an efficient passageway for water transport, while the macromolecular oil droplets were rejected on the membrane. This is because the addition of TiO_2 on SWCNTs increased the pore size and porosity of the SWCNT membrane surface, which in turn increased the permeate flux. As shown in Fig. S3 of the oil droplet size distribution of four oil-in-water emulsions, although the addition of TiO_2 increased the membrane pore diameter, it is much smaller than the smallest oil droplet size in the four oil-in-water emulsions, so that the separation effect is not diminished. Under the synthetic effect of hydrophilicity and physical blocking, water molecules are much easier to pass through the channels, while the oil droplets are obstructed outside of the membrane. Therefore, much less oil was detected in the filtrate through the SWCNT/TiO_2 membrane than SWCNT membrane. This result was also in accordance with the result of the underwater simulated oil-adhesion test as presented in Fig. 5(c) and 5(d).

Compared with other composite membranes in the literature that deal with oil-in-water emulsions, the SWCNT/TiO_2 (TiO_2/SWCNT=3) membrane exhibits excellent separation performance (Table 1)

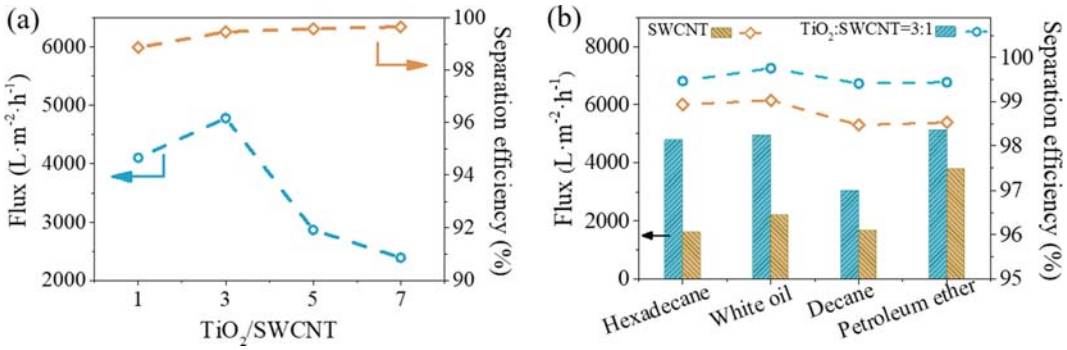

Fig. 6. (a) Permeation flux and oil-in-water separation performance of SWCNT/TiO_2 membranes. (b) Oil/water separation performance of SWCNT and SWCNT/TiO_2 membrane (TiO_2/SWCNT=3) for oil-in-water emulsions of different oil phases.

Table 1. Comparison of separation performance of SWCNT/TiO_2 (TiO_2/SWCNT=3) membrane and other composite membranes

Composite membranes	Model oil	Initial oil concentration (mg/L)	Permeation flux L/(m^2·h·bar)	Oil rejection	Ref.
PVDF/polyamide /PVA	Oil (GS-1)	100	47.5	98.5%	[30]
P(VDF-co-CTFE)-g-PMAA-g-0.136 fPEG (PVDF/AP)	Hexadecane	500	~20.59	98%	[31]
GO/TiO_2	Hexadecane	200	531	97.5%	[32]
ZrO_2-Al_2O_3	20# engine oil	1,000	316.25	97.8%	[59]
polymer@CNT	Soybean	1,000	4,592	-	[60]
silica-NPs/α-alumina tubular membrane	Cyclohexane	500	116.67	93%	[61]
CNTs-PVA	Petroleum	1,000	300	95%	[62]
nanosilica/PSF	Machine oil	65	160	98.89%	[63]
15 wt%SZY(SO_4^{2-}/ZrO_2-Y_2O_3)/PSF	Machine oil	120	55	99.16%	[64]
SWCNT/TiO_2	Hexadecane	1,500	4,777.07	99.47%	This work

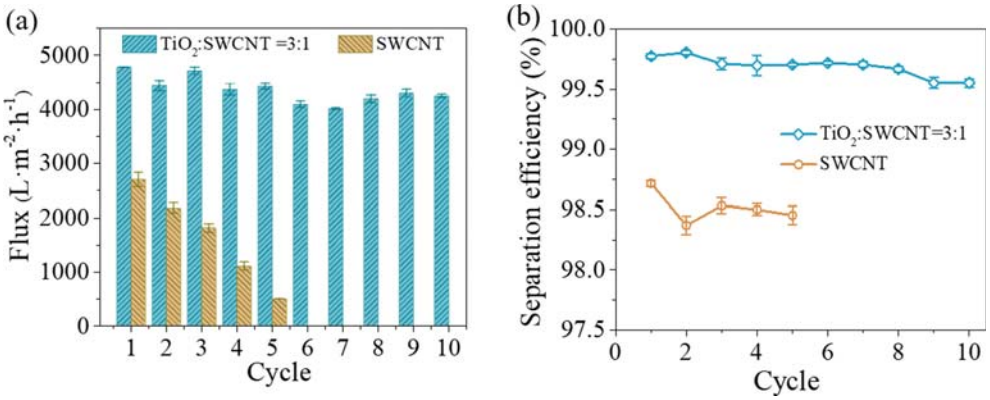

Fig. 7. Change of flux (a) and separation efficiency (b) with cycle times when separating white mineral oil-in-water emulsion by SWCNT and SWCNT/TiO_2 (TiO_2/SWCNT=3) membrane.

[30-32,59-64]. Among these studied systems, the present system has much higher initial oil concentration than that of other systems. As the initial oil concentration is 1,500 mg/L, higher permeation flux and oil rejection could be achieved by the optimal modified membrane.

Furthermore, an emulsion containing white mineral oil was prepared to evaluate the anti-fouling property of the modified membranes. It was assessed by detecting the change of the flux and separation efficiency during cyclic experiments. As observed in Fig. 7, the flux of the SWCNT membrane exhibited a continuous decreasing trend, whereas the SWCNT/TiO_2 membrane did not decrease obviously with increasing cycle number, even up to ten cycles. It can be seen that the separation efficiency of both membranes is above 98%, but that of the SWCNT/TiO_2 membrane in every cycle remains greater than 99.5%. This means that the oil content in the filtrate is less than 8 mg/L. As discussed above, the architecture of the hydrophilic TiO_2 contributed to hierarchical structures and higher water capture capacity, thus reducing the possibility of oil stain adhesion on the membrane. In addition, TiO_2 nanoparticles could polarize hydrates to form abundant surficial hydroxyl groups, which will chemically enhance anti-fouling ability. Therefore, the oil droplets have a stronger adhesion to a membrane that is not coated with TiO_2, as can be seen from underwater oil-adhesion tests in Fig. 5(c) and 5(d). This indicates the superior recyclability of the SWCNT/TiO_2 membrane, which is essential for practical applications.

CONCLUSIONS

Although SWCNT-coated membrane has a certain effect on demulsification of oil-in-water emulsions, its permeate flux and anti-fouling performance need to be further improved. TiO_2 nanoparticles contribute to the formation of hierarchical structures, polarize hydrates, and increase the porosity of the membrane surface, thus augmenting the anti-fouling ability and water transport efficiency of the membrane. With the addition of the super-hydrophilic and underwater super-oleophobic properties of the SWCNT/TiO_2 modified membrane, an ultrahigh permeation flux of up to 4,777.07 L·m^{-2}·h^{-1} was achieved, which is one order of magnitude higher than commercial filtration membranes with similar oil rejection properties. The membrane has excellent oil-in-water separation performance with efficiency greater than 99.47%. More importantly, the modified membrane maintains high separation capacity even after

ten cycles and the oil fouling in the membrane can be cleaned by simple water cleaning, indicating the excellent antifouling property of the membrane. Therefore, we expect that this study would be beneficial for the separation of oil-in-water emulsions by microfiltration processes.

ACKNOWLEDGEMENTS

This work was supported by the National Natural Science Foundation of China (grant no. 21677087) and the National Science and Technology Major Project of China (grant no. 2016ZX05040-005). The author thanks Jake Carpenter from UCLA for linguistic assistance.

SUPPORTING INFORMATION

Additional information as noted in the text. This information is available via the Internet at http://www.springer.com/chemistry/journal/11814.

REFERENCES

1. W. Zhang, Y. Zhu, X. Liu, D. Wang, J. Li, L. Jiang and J. Jin, *Angew. Chem.*, **53**, 856 (2014).
2. X. Yue, J. Li, T. Zhang, F. Qiu, D. Yang and M. Xue, *Chem. Eng. J.*, **328**, 117 (2017).
3. S. Zhang, P. Wang, X. Fu and T. S. Chung, *Water Res.*, **52**, 112 (2014).
4. P. Kajitvichyanukul, Y. T. Hung and L. K. Wang, *Handbook of environmental engineering*, Humana Press, Totowa (2011).
5. M. A. Shannon, P. W. Bohn, M. Elimelech, J. G. Georgiadis, B. J. Mariñas and A. M. Mayes, *Nature*, **452**, 301 (2008).
6. Z. Li, T. Shi, T. Zhang, Q. Guo, F. Qiu, X. Yue and D. Yang, *Korean J. Chem. Eng.*, **36**, 92 (2019).
7. X. Hu, Y. Yu, J. Zhou, Y. Wang, J. Liang, X. Zhang, Q. Chang and L. Song, *J. Membr. Sci.*, **476**, 200 (2015).
8. A. K. Fard, T. Rhadfi, G. Mckay, M. Al-marri, A. Abdala, N. Hilal and M. A. Hussien, *Chem. Eng. J.*, **293**, 90 (2016).
9. B. Das, B. Chakrabarty and P. Barkakati, *Korean J. Chem. Eng.*, **34**, 2559 (2017).
10. C. Ong, Y. Shi, J. Chang, F. Alduraiei, N. Wehbe, Z. Ahmed and P. Wang, *Sep. Purif. Technol.*, **227**, 115657 (2019).
11. B. Chakrabarty, A. K. Ghoshal and M. K. Purkait, *J. Membr. Sci.*, **325**, 427 (2008).
12. F. Zhang, W. Zhang, Z. Shi, D. Wang, J. Jin and L. Jiang, *Adv. Mater.*, **25**, 4192 (2013).
13. W. Zhang, N. Liu, Y. Cao, X. Lin, Y. Liu and L. Feng, *Adv. Mater. Interfaces*, **4**, 1600029 (2017).
14. V. Rajakovic-Ognjanovic, G. Aleksic and L. Rajakovic, *J. Hazard. Mater.*, **154**, 558 (2008).
15. L. Liu, J. Lei, L. Li, R. Zhang, N. Mi, H. Chen, D. Huang and N. Li, *Mater. Lett.*, **195**, 66 (2017).
16. Z. Wang, D. Wang, Z. Li and Y. Wang, *Cellulose*, **27**, 2427 (2016).
17. R. Liu, X. Li, H. Liu, Z. Luo, J. Ma, Z. Zhang and Q. Fu, *RSC Adv.*, **6**, 30301 (2016).
18. A. Salahi, T. Mohammadi, R. M. Behbahani and M. Hemmati, *Korean J. Chem. Eng.*, **32**, 1101 (2015).
19. L. Wang, S. Ji, N. Wang, R. Zhang, G. Zhang and J. R. Li, *J. Membr. Sci.*, **452**, 143 (2014).
20. A. K. Basumatary, R. V. Kumar, A. K. Ghoshal and G. Pugazhenthi, *J. Membr. Sci.*, **475**, 521 (2015).
21. H. Adib, S. Hassanajili, M. R. Sheikhi-Kouhsar, A. Salahi and T. Mohammadi, *Korean J. Chem. Eng.*, **32**, 159 (2015).
22. L. Du, X. Quan, X. Fan, S. Chen and H. Yu, *Sep. Purif. Technol.*, **210**, 891 (2019).
23. A. K. Kota, G. Kwon, W. Choi, J. M. Mabry and A. Tuteja, *Nat. Commun.*, **3**, 1025 (2012).
24. F. Li, R. Gao, T. Wu and Y. Li, *J. Membr. Sci.*, **543**, 163 (2017).
25. M. B. Ghandashtani, F. Z. Ashtiani, M. Karimi and A. Fouladitajar, *Appl. Surf. Sci.*, **349**, 393 (2015).
26. H. Shi, Y. He, Y. Pan, D. Haihui, G. Zeng, L. Zhang and C. Zhang, *J. Membr. Sci.*, **506**, 60 (2016).
27. A. Hong, A. G. Fane and R. Burford, *J. Membr. Sci.*, **222**, 19 (2003).
28. T. Kawakatsu, R. M. Boom, H. Nabetani, Y. Kikuchi and M. Nakajima, *AIChE J.*, **45**, 967 (1999).
29. J. Kong and K. Li, *Sep. Purif. Technol.*, **16**, 83 (1999).
30. S. Wang, L. Chu and W. Chen, *Chin. J. Chem. Eng.*, **14**, 37 (2006).
31. X. Zhu, W. Tu, K. H. Wee and R. Bai, *J. Membr. Sci.*, **466**, 36 (2014).
32. Z. Wu, Z. Chang, K. Peng, Q. Wang and Z. Wang, *Front. Env. Sci. Eng.*, **12**, 1 (2018).
33. S. J. Gao, H. Qin, P. Liu and J. Jin, *J. Mater. Chem. A*, **3**, 6649 (2015).
34. M. M. Pendergast and E. M. V. Hoek, *Energy Environ. Sci.*, **4**, 1946 (2011).
35. J. Sun, M. Iwasa, L. Gao and Q. Zhang, *Carbon*, **42**, 895 (2004).
36. J. Gu, P. Xiao, J. Chen, J. Zhang, Y. Huang and T. Chen, *ACS Appl. Mater. Interfaces*, **6**, 16204 (2014).
37. M. Grujicic, B. Pandurangan, D. C. Angstadt, K. L. Koudela and B. A. Cheeseman, *J. Mater. Sci.*, **42**, 5347 (2007).
38. A. Kalra, S. Garde and G. Hummer, *Proc. Natl. Acad. Sci. USA*, **100**, 10175 (2003).
39. W. J. Ma, L. Song, R. Yang, T. H. Zhang, Y. C. Zhao, L. F. Sun, Y. Ren, D. F. Liu, L. F. Liu, J. Shen, Z. X. Zhang, Y. J. Xiang, W. Y. Zhou and S. S. Xie, *Nano Lett.*, **7**, 2307 (2007).
40. I. E. Palamà, S. D'Amone, M. Biasiucci, G. Gigli and B. Cortese, *J. Mater. Chem. A*, **2**, 17666 (2014).
41. X. Yue, T. Zhang, D. Yang, F. Qiu and Z. Li, *Ind. Eng. Chem. Res.*, **57**, 10439 (2018).
42. V. Vatanpour, S. S. Madaeni, R. Moradian, S. Zinadini and B. Astinchap, *Sep. Purif. Technol.*, **90**, 69 (2012).
43. S. M. Abdelbasir and A. E. Shalan, *Korean J. Chem. Eng.*, **36**, 1209 (2019).
44. Y. L. Thuyavan, N. Anantharaman, G. Arthanareeswaran, A. F. Ismail and R. V. Mangalaraja, *Desalination*, **365**, 355 (2015).
45. A. Fujishima, X. Zhang and D. A. Tryk, *Surf. Sci. Rep.*, **63**, 515 (2008).
46. H. G. Yang, C. H. Sun, S. Z. Qiao, J. Zou, G. Liu, S. C. Smith, H. M. Cheng and G. Q. Lu, *Nature*, **453**, 638 (2008).
47. S. J. Gao, Z. Shi, W. B. Zhang, F. Zhang and J. Jin, *ACS Nano*, **8**, 6344 (2014).
48. F. Shi, Y. Ma, J. Ma, P. Wang and W. Sun, *J. Membr. Sci.*, **389**, 522 (2012).
49. A. I. López-Lorente, B. M. Simonet and M. Valcárcel, *Anal. Chem.*, **82**, 5399 (2010).
50. R. Moradian and B. Astinchap, *Nano*, **5**, 139 (2010).

51. M. Adeli, A. Bahari and H. Hekmatara, *Nano*, **3**, 37 (2008).
52. J. Zhou, X. Zhou, X. Sun, R. Li, M. Murphy, Z. Ding, X. Sun and T. K. Sham, *Chem. Phys. Lett.*, **437**, 229 (2007).
53. Y. Ying, J. C. Yu, J. G. Yu, Y. C. Kwok, Y. K. Che, J. C. Zhao, D. Lu, W. K. Ge and P. K. Wong, *Appl. Catal. A-Gen.*, **289**, 186 (2005).
54. X. Li, J. Niu, Z. Jin, H. Li and Z. Liu, *J. Phys. Chem. B*, **107**, 2453 (2003).
55. R. N. Wenzel, *Ind. Eng. Chem.*, **28**, 988 (1936).
56. T. Yuan, J. Meng, T. Hao, Y. Zhang and M. Xu, *J. Membr. Sci.*, **470**, 112 (2014).
57. P. Gao, Z. Liu, D. D. Sun and W. J. Ng, *J. Mater. Chem. A*, **2**, 14082 (2014).
58. X. Peng, J. Jin, N. Yoshimichi, O. Takahisa and I. Izumi, *Nat. Nanotechnol.*, **4**, 353 (2009).
59. J. Zhou, Q. Chang, Y. Wang, J. Wang and G. Meng, *Sep. Purif. Technol.*, **75**, 243 (2010).
60. Y. Liu, Y. Su, J. Cao, J. Guan, R. Zhang, M. He, L. Fan, Q. Zhang and Z. Jiang, *J. Membr. Sci.*, **542**, 254 (2017).
61. R. Liu, A. K. Y. Raman, I. Shaik, C. Aichele and S.-J. Kim, *J. Water Process Eng.*, **26**, 124 (2018).
62. M. Tian, Y. Liao and R. Wang, *J. Membr. Sci.*, **596**, 1 (2020).
63. Y. Zhang, L. Shan, Z. Tu and Y. Zhang, *Sep. Purif. Technol.*, **63**, 207 (2008).
64. Y. Zhang, C. Ping, T. Du, L. Shan and Y. Wang, *Sep. Purif. Technol.*, **70**, 153 (2009).

Supporting Information

Superwetting TiO_2-decorated single-walled carbon nanotube composite membrane for highly efficient oil-in-water emulsion separation

Yahong Sun*, Ruiguang Zhao, Quanyong Wang***, Yuanyuan Zheng*, Gongrang Li****, Dejun Sun**, Tao Wu**,†, and Yujiang Li*,†**

*Shandong Provincial Research Center for Water Pollution Control, School of Environmental Science and Engineering, Shandong University, Jinan, 250100, P. R. China
**Key Laboratory of Colloid and Interface Science of Education Ministry, Shandong University, Jinan, 250100, P. R. China
***China Urban Construction Design & Research Institute Co. LTD. Jinan, 250101, P. R. China
****Drilling Technology Research Institute, Shengli Petroleum Engineering Corporation Limited of SINOPEC, Dongying, 257017, P. R. China
(*Received 5 January 2020 • Revised 9 May 2020 • Accepted 20 May 2020*)

Table S1. Comparison of separation effects of several adsorbents and membrane materials

Materials	Oil removal efficiency/ oil adsorption capacity	Recyclability	Ref.
Inorganic sorbents	19.6%-21.2%	-	[14]
Organic sorbents	43%-95%	-	[14]
Sponge	25-87 times its own weight	5 cycles	[15]
Natural fiber materials	85.2%	8 cycles	[16]
Aerogel	22-87 times its own weight	5 cycles	[17]
Membrane	99.75%	10 cycles	This work

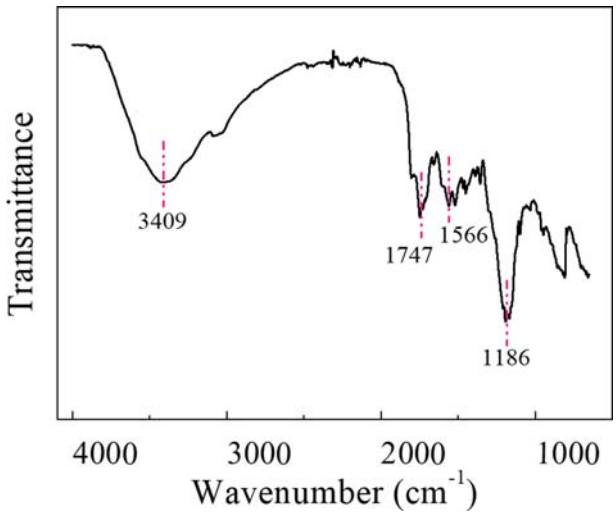

Fig. S1. ATR-FTIR spectra of SWCNTs particles.

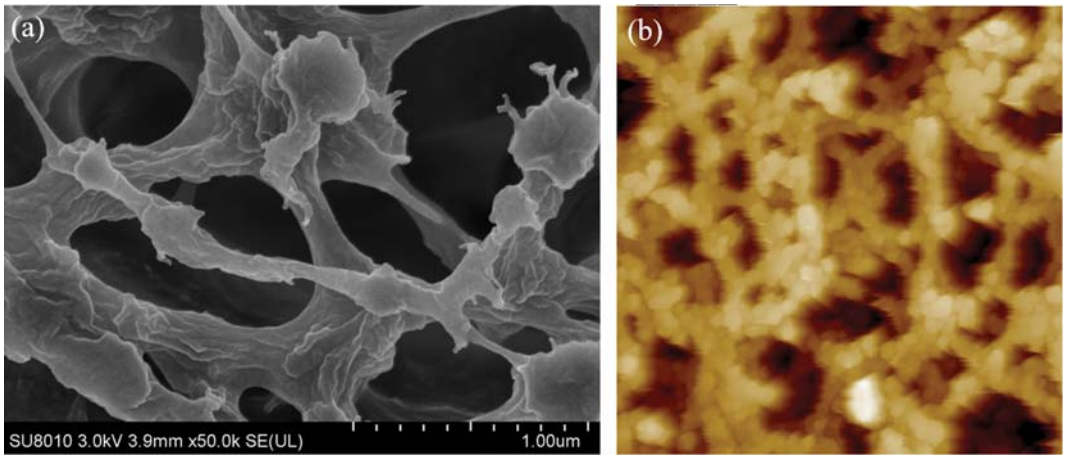

Fig. S2. SEM image (a) and AFM image (b) of pure CA membrane.

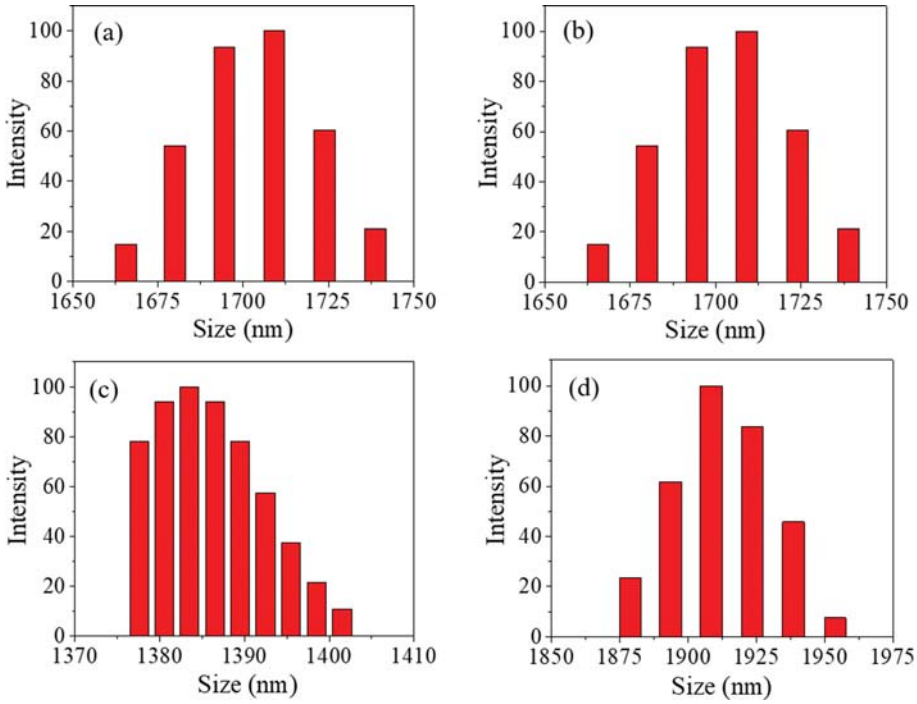

Fig. S3. Oil droplet size distribution of the SDBS-stabilized oil-in-water emulsion, including (a) hexadecane-in-water, (b) white mineral oil-in-water, (c) decane-in-water, and (d) petroleum ether-in-water was examined by DLS.